

## NO<sub>x</sub> Conversion of Porous LSF<sub>15</sub>-CGO<sub>10</sub> Cell Stacks

A.Z. Friedberg and K. Kammer Hansen\*

Department of Energy Conversion and Storage, Technical University of Denmark  
Frederiksborgvej 399, DK-4000, Roskilde, Denmark

Received: November 27, 2014, Accepted: February 25, 2015, Available online: April 20, 2015

**Abstract:** A porous electrochemical reactor, made of La<sub>0.85</sub>Sr<sub>0.15</sub>FeO<sub>3</sub> as electrode and Ce<sub>0.9</sub>Gd<sub>0.1</sub>O<sub>1.95</sub> as electrolyte, was studied for the electrochemical reduction of NO with Propene. In order to enhance the effect of polarization, the reactor was impregnated with Ce<sub>0.9</sub>Gd<sub>0.1</sub>O<sub>1.95</sub>, CeO<sub>2</sub> or Ce<sub>0.8</sub>Pr<sub>0.2</sub>O<sub>2-d</sub> nanoparticles. The HC-SCR on the cells was increased on the impregnated cells, but no electrochemical enhancement of this was observed. The applied overpotential on the impregnated cells changed the oxidation reaction of NO into NO<sub>2</sub> which is considered an intermediate in the NO reduction to nitrogen.

Keywords:

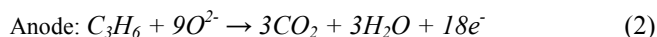
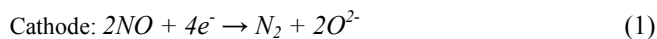
### 1. INTRODUCTION

The exhaust of lean burn engines contain excess oxygen which eliminates the use of the three way catalytic converter for the NO<sub>x</sub> removal [1]. The urea-based selective catalytic reduction (SCR) is one of the most promising technologies for removal of NO from lean burn engine exhaust. The SCR system however is dependent on a reducing agent causing some concerns in terms of storage, distribution infrastructure and potential freezing of the urea solution [2]. In 1991, Iwamoto and Hamada [3] introduced the selective reduction of NO by hydrocarbons in the presence of oxygen. Since then many studies have been conducted in this field also on perovskite type materials [4–6]. The activity of the reaction is however too low for commercial use since the reduction of oxygen in the gas is a competing reaction. Pancharatnam et al. [7] discovered in 1975 the electrochemical reduction of NO and this technology is a very good alternative to SCR because no reducing agent is needed. Since then many has investigated different materials for cathodes, and several reviews has been published on this subject [8–11].

Also perovskites has been studied for the electrochemical reduction of NO [10, 12–19]. The strontium doped lanthanum ferrite, (LSF) was investigated in air, and La<sub>0.85</sub>Sr<sub>0.15</sub>FeO<sub>3</sub> (LSF<sub>15</sub>) showed to have the highest activity of the La<sub>1-x</sub>Sr<sub>x</sub>FeO<sub>3-d</sub> (LSF) in air. Further, Fe(III) seems to be the catalytic active specie [20]. Later it

was shown that LSF have a higher activity towards the electrochemical reduction of nitric oxide than towards the electrochemical reduction of oxygen [15]. Werchmeister et al. [17] used a ceramic electrochemical reactor, with a composite electrode consisting of strontium doped manganite (LSM<sub>15</sub>) and ceria doped with gadolinium (CGO<sub>10</sub>), and CGO<sub>10</sub> electrolyte. They showed that impregnation with ceria, CGO<sub>10</sub> and ceria doped with praseodymium (CPO<sub>20</sub>) nanoparticles of the porous reactor structure cell was necessary for NO decomposition to take place. Up to 35% NO could be removed without the presence of oxygen. Later, it was shown that the electrochemical oxidation of propene on LSM<sub>15</sub>/CGO<sub>10</sub> and LSF<sub>15</sub>/CGO<sub>10</sub> electrodes could be greatly enhanced by CeO<sub>2</sub>, CGO<sub>10</sub> and CPO<sub>20</sub> impregnation of nanoparticles. [21, 22].

In this work the electrochemical reduction of NO is studied on LSF<sub>15</sub>/CGO<sub>10</sub> electrodes in a porous electrochemical reactor. The effect of propene on the NO decomposition is investigated, and the improvement of the selectivity and activity of the electrodes is done by impregnation of CeO<sub>2</sub>, CGO<sub>10</sub>, and CPO<sub>20</sub>. The desired reactions occurring under polarisation is the reduction on NO to N<sub>2</sub> at the cathode, (Eq. 1), and the oxidation of propene to CO<sub>2</sub> and H<sub>2</sub>O at the anode (Eq. 2).



The oxygen reduction reaction at the cathode (Eq. 3) is a com-

\*To whom correspondence should be addressed: Email: kkha@dtu.dk  
Phone:

peting reaction, which is the drawback of this method, and the reason for why the selectivity of the cathode is important.



## 2. EXPERIMENTAL

### 2.1. Fabrication of cell and impregnation

The electrochemical cells used in this study, consisted of 11 alternating layers of electrode and electrolyte material. The 11 layer makes 5 single cells in a stack. The electrolyte and electrode were ceramic materials and the electrolyte tape was made of  $\text{Ce}_{0.9}\text{Gd}_{0.1}\text{O}_{1.95}$  (CGO<sub>10</sub>) purchased from Rhodia. The electrode was made of 35 wt% CGO<sub>10</sub> and 65 wt%  $\text{La}_{0.85}\text{Sr}_{0.15}\text{FeO}_3$  (LSF<sub>15</sub>) purchased from American Elements. The LSF<sub>15</sub> and CGO<sub>10</sub> powder were mixed with binder, dispersant and graphite as pore former. The electrode slurries were ball milled and then tape-casted. The CGO<sub>10</sub> electrolyte was made in the same way as the electrode tape. The tapes were laminated together to create 11 alternating layers (of electrode and electrolyte, 5 single cells in series, a porous cell stack) and round cells were stamped with a diameter of 18 mm. The cells were sintered at 1250 °C for 2 h. During the sintering the cells shrunk to 14.5 mm in diameter and the graphite was burned off creating the porous structure through the cell. For a detailed description of porous cell stack fabrication, see Andersen et al. [23].

The cells were painted on both sides with a gold paste mixed with 20 wt% graphite and hereafter calcined at 800 °C to decompose the graphite creating a porous current collector. Some of the cells were impregnated with ceria, CGO<sub>10</sub> or CPO<sub>20</sub> nanoparticles. Aqueous solutions of 3 M of the respective nitrates from Alfa Aesar were prepared using 10 wt% P123 (BASF) as surfactant and Milipore water. For the CGO<sub>10</sub> solution, 10 mol%  $\text{Gd}(\text{NO}_3)_3$  and 90 mol%  $\text{Ce}(\text{NO}_3)_3$  were used, and for the CPO<sub>20</sub> solution 20 mol%  $\text{Pr}(\text{NO}_3)_3$  and 80 mol%  $\text{Ce}(\text{NO}_3)_3$  were used. The cells were impregnated by covering them with the solution and placing them at 0.1 mbar vacuum for 10 sec. The cells were heated to 350 °C to decompose the surfactant. The weight of the cells was 0.19 g for the non-impregnated and 0.24 g, 0.25 g and 0.23 g for the Ceria, CGO<sub>10</sub> and CPO<sub>20</sub> impregnated cells, respectively. The cells were impregnated three times and gained approximately 13% by weight.

### 2.2. Test set-up

A cell stack was placed between two alumina tubes inside a glass tube in a one atmosphere set-up. Figure 1 illustrates the set-up showing the gas flow through the porous structure of the cell. The atmosphere at the anode and cathode sides of the cells is not separated. In this set-up the sides of the cell stack are not sealed, which means that the gas is not forced through the cell stack and it is possible for some of the gas to avoid getting into contact with all the layers of the cell.

The gas flow of 2 L/h was provided by Brooks mass flow controllers. The composition of the atmosphere was 1000 ppm NO (Air Liquid; 1% ±0.02% NO in Ar) + 10% O<sub>2</sub> (Air Liquide; 20% O<sub>2</sub> ±2% Ar) in Ar or 1000 ppm NO (Air Liquid; 1% ±0.02% NO in Ar) + 1000 ppm C<sub>3</sub>H<sub>6</sub> (Air Liquide; 1% ±0.02% C<sub>3</sub>H<sub>6</sub> in Ar) + 10% O<sub>2</sub> (Air Liquide; 20% O<sub>2</sub> ±2% Ar) in Ar. The set-up was placed in a small vertical furnace, which allowed the temperature to be controlled. The composition of the gas outlet was monitored and rec-

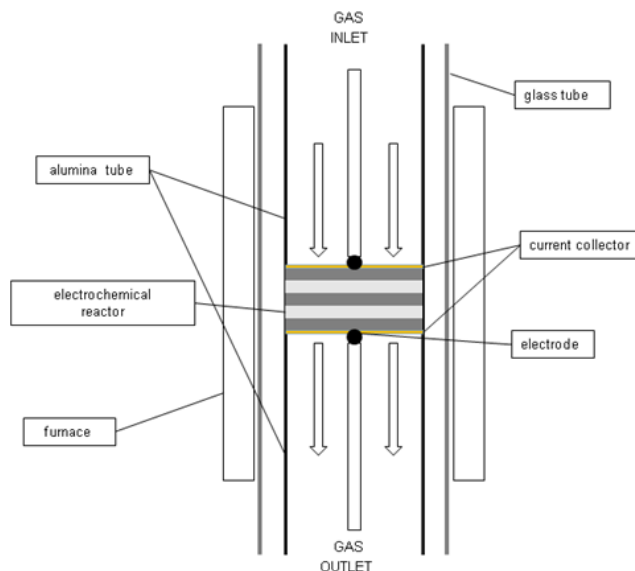


Figure 1. Scheme of the set-up for testing on porous cell stacks

orded by a chemiluminescence detector (Model 42i HL, Thermo Scientific, USA) for NO and NO<sub>2</sub>. The C<sub>3</sub>H<sub>6</sub>, CO, CO<sub>2</sub> and N<sub>2</sub>O concentrations were monitored by a Agilent 6890 N gas chromatograph, equipped with Hayesep N and Molesieve 13X columns and a thermal conductivity detector. The nitrogen was estimated from a mass balance of NO, NO<sub>2</sub> and N<sub>2</sub>O.

### 2.3. Electrochemical measurements

For the electrochemical studies of the cells, a potentiostat (Gamry, reference 600 USA) was used. The characterization was done by recording electrochemical impedance spectra in the frequency range 878787 Hz to 0.0013 Hz. The recording was done at open circuit voltage (OCV) with a root mean square amplitude of 36 mV and 6 points per decade. All the experiments started with a recording of an impedance spectra followed by half an hour at OCV. Hereafter 2 hours of chronoamperometry was performed with an anodic potential of +3 V with respect to OCV. Then the cell was kept at OCV for 30 min until it was stable, and a cathodic potential of -3 V was applied to the cells. Cyclic voltammetry was also performed on the cell stacks. A sweep rate of 10 mV/s was used with a range of -3 V to +3 V relative to OCV. First, the cell was characterized at a temperature of 300 °C in an atmosphere of 1000 ppm NO + 10% O<sub>2</sub>. The temperature was then increased and the test repeated at 350 and 400 °C. Then the gas was switched to a composition of 1000 ppm NO + 1000 ppm C<sub>3</sub>H<sub>6</sub> + 10% O<sub>2</sub>. The electrochemical characterization was performed again at the same temperatures as before. The test procedure prevented the cell from getting contaminated by carbon, before it had been evaluated in the propene free atmosphere. The impedance data were analysed with the open source software, Elchemea Analytical [24]. Kramer-Kronig transformation was used for the validation of all impedance spectra.

### 2.4. Scanning electron microscopy

The microstructure of the electrochemical cells were examined

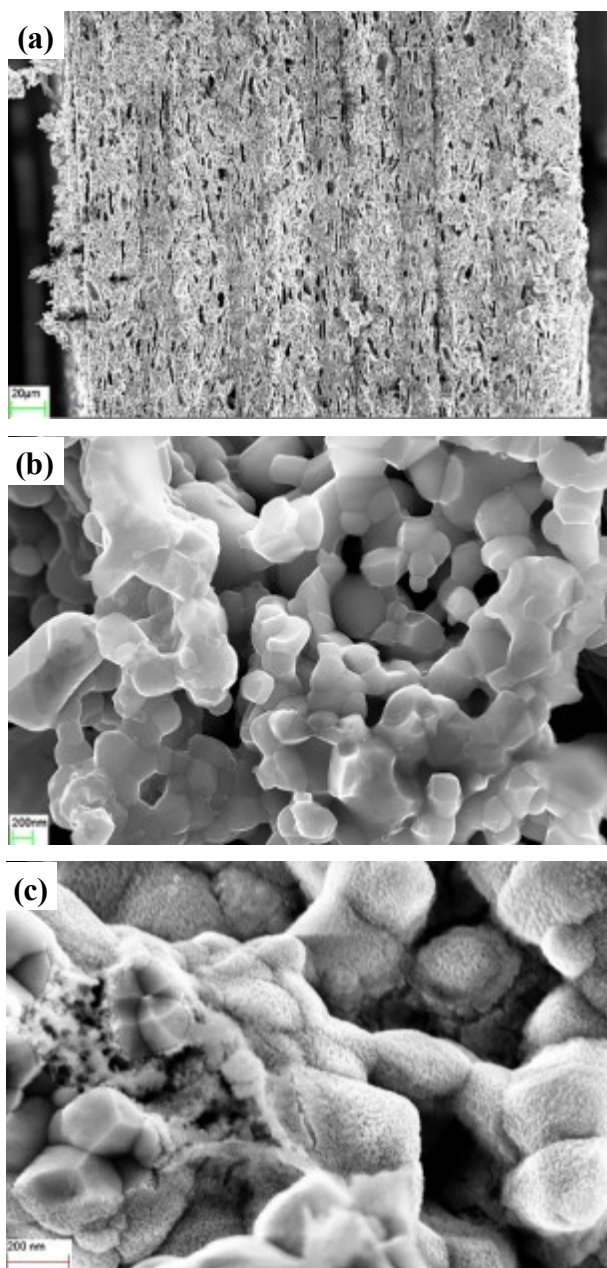


Figure 2. Scanning electron microscopy images of cell stacks and impregnation material in the porous structure. (a) 11 layers cell stack, (b) Electrode layer of a non impregnated cell stack, (c) Outer electrode of a CGO<sub>10</sub> impregnated cell stack. nanoparticles of impregnation material is sitting on the LSF particles

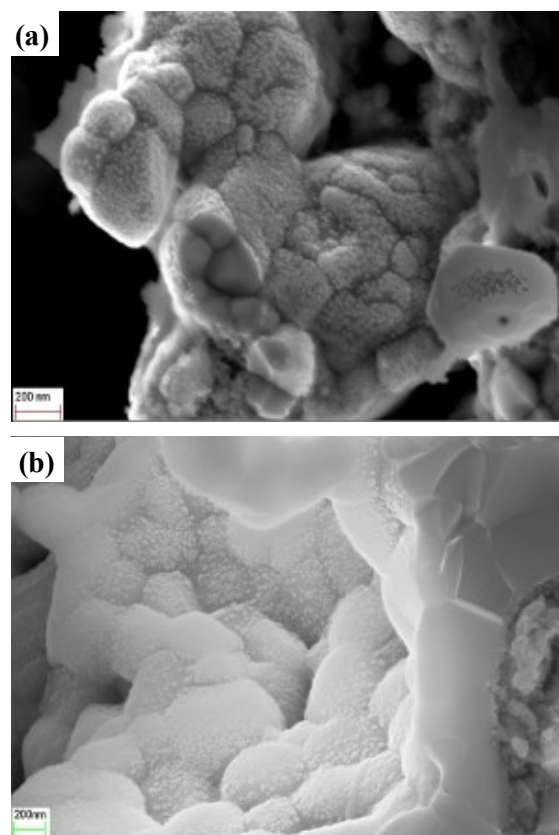


Figure 3. Scanning electron microscopy images of impregnation in the porous structure of cell stacks. (a) Inner electrode of a cell stack with CPO<sub>20</sub> impregnation, (b) Outer electrode of a Ceria impregnated cell stack

by scanning electron microscopy (SEM) using a Zeiss Supra 35 microscope. The samples were broken into fitting pieces of approximately 5 × 5 mm, and put directly into the microscope. The SEM images were recorded with an in-lens detector with an acceleration voltage of 5 keV. The cells were examined after testing.

### 3. RESULTS

#### 3.1. Structural Characterization

SEM images of the cell stacks investigated are shown in figure 2 and 3. In Fig. 2(a) the 11 layers of the cell is shown where the composite electrode (bright) and the electrolyte (dark) layers can be seen together with the gold current collector sitting on the sides of the cell. The impregnation method was efficient and the nanoparticles were found throughout the cell porosity (compare figure 2(b) and figure 2(c)-3(b)).

Table 1. Catalytic conversion of NO<sub>x</sub> on the four 11 layers porous cell stacks in 1000 ppm NO + 10% O<sub>2</sub>. NI: Non impregnated.

	300		370		400	
	NO + O <sub>2</sub>	NO + C <sub>3</sub> H <sub>6</sub> + O <sub>2</sub>	NO + O <sub>2</sub>	NO + C <sub>3</sub> H <sub>6</sub> + O <sub>2</sub>	NO + O <sub>2</sub>	NO + C <sub>3</sub> H <sub>6</sub> + O <sub>2</sub>
NI	3%	5%	4%	7%	5%	4%
CPO <sub>20</sub>	5%	10%	3%	9%	3%	8%
Ceria	4%	7%	0%	8%	0%	6%
CGO <sub>10</sub>	4%	9%	2%	10%	1%	9%

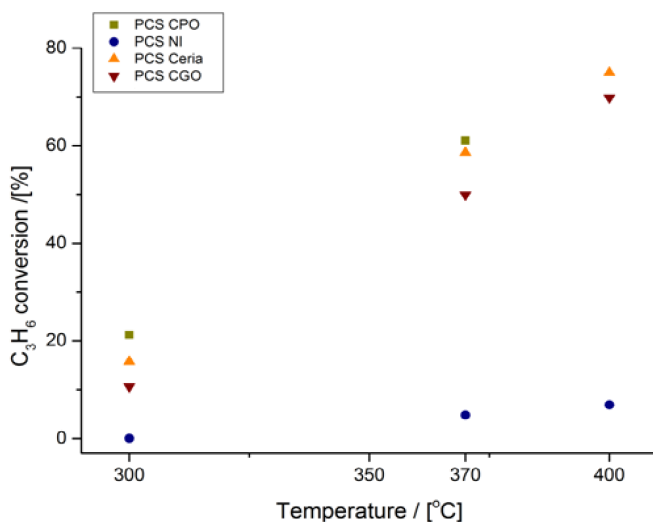


Figure 4. Propene conversion versus temperature on non impregnated (NI), CPO<sub>20</sub>, CGO<sub>10</sub> or Ceria impregnated cell stacks. Gas feed: 1000 ppm NO + 1000 ppm C<sub>3</sub>H<sub>6</sub> + 10% O<sub>2</sub>

### 3.2. Catalytic activity

Very little catalytic conversion of NO<sub>x</sub> into nitrogen was seen on the porous cell stack in 1000 ppm NO + 10% O<sub>2</sub> atmosphere (see table 1). The conversion of NO<sub>x</sub> on all the cells increased when propene was added to the atmosphere. The CPO<sub>20</sub> and CGO<sub>10</sub> impregnated cell stack seemed very alike in the catalytic activity. It was possible to remove up to approximately 10% of NO on these cells. At no time N<sub>2</sub>O was detected. At OCV the concentration of NO and NO<sub>2</sub> was very different in the test on the non-impregnated cell stack compared to the impregnated cells. In 1000 ppm NO + 10% O<sub>2</sub> the concentration of NO<sub>2</sub> exceeded that of NO in the test done on the impregnated cell stacks at 350 and 400 °C. At 300 °C and on the non-impregnated cell stack very little NO<sub>2</sub> was present in the atmosphere. When propene was added to the atmosphere the NO concentration was always higher than NO<sub>2</sub> at OCV. The CPO<sub>20</sub> impregnated cell was the best catalyst for the oxidation of NO into NO<sub>2</sub>, and CGO<sub>10</sub> and ceria were very similar. The non-impregnated cell was the least active catalyst towards this reaction.

Figure 4 shows the conversion of propene into CO<sub>2</sub> at different temperatures for the non-impregnated backbone and the impregnated cells measured at OCV. The propene conversion reached by the CGO<sub>10</sub> and Ceria impregnated cells, were 69% and 75% at 400 °C, respectively; the backbone reached 7% at the same temperature. The CPO<sub>20</sub> impregnated cell stack showed higher catalytic conversion of propene at 300 and 350 °C than all the other cells. It was clear that the impregnation materials were able to strongly increase the catalytic activity of the cell towards propene oxidation. The selectivity to CO<sub>2</sub> for all the cells was 100% at all temperatures since no CO was detected at any time.

### 3.3. Electrochemical conversion

No effect of polarization on the NO<sub>x</sub> conversion into nitrogen was observed on any of the cells, but the ratio between the NO and NO<sub>2</sub> concentration in the atmosphere changed considerably when a

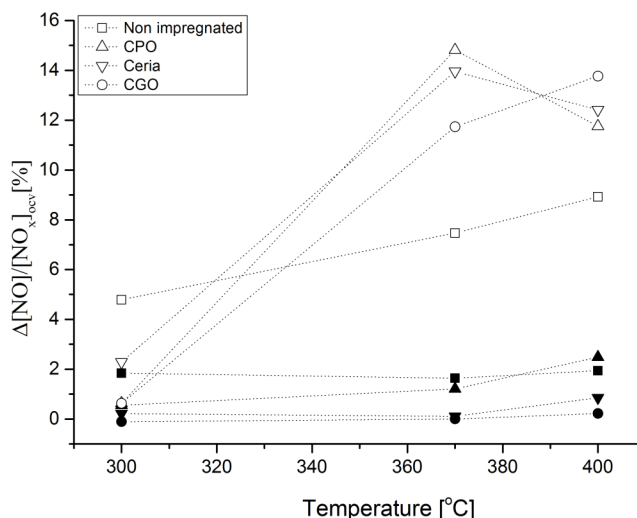


Figure 5. Relative conversion of NO during cathodic polarisation of -3 V on non-impregnated cell and impregnated cell stacks supplied with 1000 ppm NO + 10% O<sub>2</sub> (open) and 1000 ppm NO + 1000 ppm C<sub>3</sub>H<sub>6</sub> + 10% O<sub>2</sub> (solid)

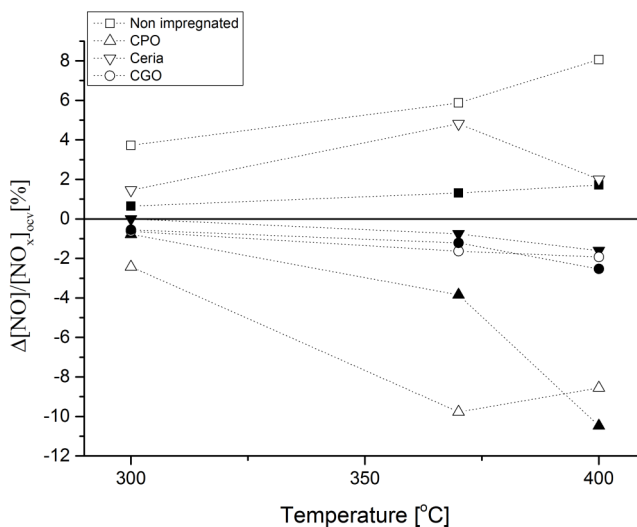


Figure 6. Relative conversion of NO during anodic polarisation of +3 V on non-impregnated cell and impregnated cell stacks supplied with 1000 ppm NO + 10% O<sub>2</sub> (open) and 1000 ppm NO + 1000 ppm C<sub>3</sub>H<sub>6</sub> + 10% O<sub>2</sub> (solid) Negative values correspond to removal of NO and positive to formation of NO

potential was applied to the cells. The behaviour of these gasses was very different and dependent on impregnation material (see figure 5 and 6). The test done on the non-impregnated and the ceria impregnated cell stack, showed the same behaviour of NO and NO<sub>2</sub> in 1000 ppm NO + 10 % O<sub>2</sub>. The NO concentration increased during polarization both when cathodic and anodic potential was applied and the effect of the positive polarization was greatest. When propene was added to the atmosphere the non-impregnated cell

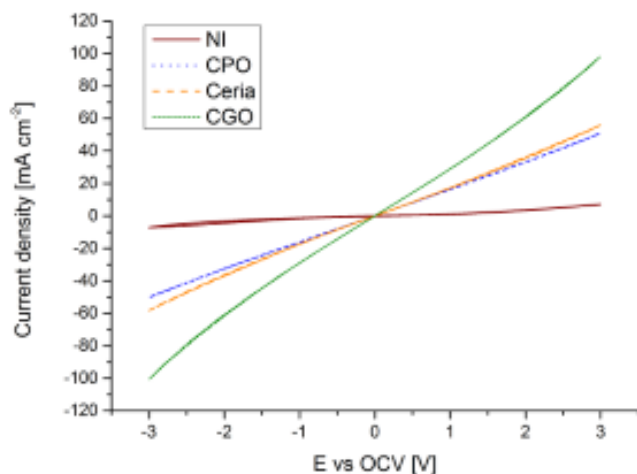


Figure 7. Cyclic voltammogram for LSF<sub>15</sub>GCO<sub>10</sub> electrodes impregnated with CPO<sub>20</sub>, CGO<sub>10</sub> or Ceria and a non-impregnated (NI) in 1000 ppm NO + 10% O<sub>2</sub> at 370 °C

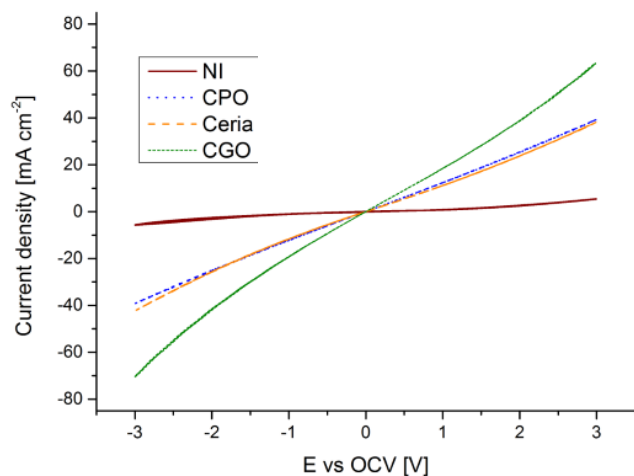


Figure 8. Cyclic voltammogram for LSF<sub>15</sub>GCO<sub>10</sub> electrodes impregnated with CPO<sub>20</sub>, CGO<sub>10</sub> or Ceria and a non-impregnated (NI) in 1000 ppm NO 1000 ppm C<sub>3</sub>H<sub>6</sub>+ 10% O<sub>2</sub> at 370 °C

stack showed no change in behaviour, but the ceria impregnated one, showed sensitivity towards polarization direction. When the cell was polarized negative, i.e. the top electrode exposed to the gas stream becomes a cathode, the NO concentration decreased. The test done on CPO<sub>20</sub> and CGO<sub>10</sub> impregnated cell stacks showed similar behaviour of the NO and NO<sub>2</sub> concentrations but the polarization effect was more significant on the CPO<sub>20</sub> impregnated cell stack. In the atmosphere without propene, the cells were sensitive to the polarization direction. When polarized anodic the NO concentration increased and when polarised cathodic it decreased. This behaviour was seen in both atmospheres.

The polarisation effect of propene conversion on the cell stack was low and the conversion only increased with a few percent at all temperatures on the three impregnated cells and no enhancement was seen on the non impregnated cell stack. Up to 77% of propene

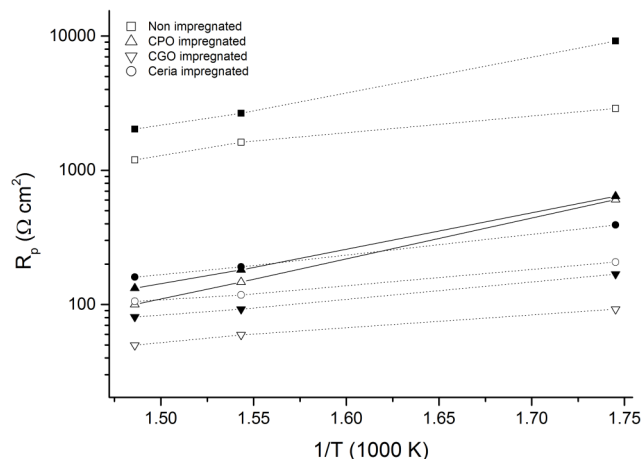


Figure 9. Arrhenius plot of polarisation resistance for the four cell stacks. Data obtained in 1000 ppm NO + 1000 ppm C<sub>3</sub>H<sub>6</sub> + 10% O<sub>2</sub>(solid) and in 1000 ppm NO + 10% O<sub>2</sub>(open)

was removed on the ceria impregnated cell at 400 °C during both anodic and cathodic polarisation.

The cyclic voltammograms for the four cells in the two different atmospheres at 370 °C are shown in figure 7 and 8. The current density decreased with decreasing temperature for all the cells in both atmospheres and it was higher in the atmosphere without propene. The least active cell was as expected the non-impregnated one, and CGO<sub>10</sub> showed the highest current density whereas the CPO<sub>20</sub> and ceria were very similar.

### 3.4. Electrochemical Impedance Spectroscopy

The impedance spectra obtained in 1000 ppm NO + 10% O<sub>2</sub> could be fitted with an ohmic resistance in series with three sub circuits consisting of RQ-elements. An RQ element is a resistance in parallel with a constant phase element with the following impedance:

$$Z = 1/(Y_0 (j \omega)^n) \quad (4)$$

where  $Y_0$  is the amplitude,  $n$  is the frequency exponent and  $w$  is the angular frequency. When propene was added to the atmosphere four sub circuits were used to get a satisfying fit of the model for the spectra obtained at 370 and 400 °C on the non-impregnated cell stack. An Arrhenius plot of the polarisation resistance ( $R_p$ ) for the cell stacks in the two different atmospheres is shown in figure 9. As can be seen, the  $R_p$  for the CPO<sub>20</sub> and ceria impregnated cells are very close but at low temperature the ceria impregnated cell is easier to polarise, where this is opposite at higher temperature where the CPO<sub>20</sub> impregnated cell stack show a lower  $R_p$ . The cell stack

Table 2. Activation energies for the cell stacks; Non impregnated (NI) or impregnated with CPO<sub>20</sub>, CGO<sub>10</sub> or Ceria.

		CPO <sub>20</sub>	NI	CGO <sub>10</sub>	Ceria
E <sub>a</sub>	NO + O <sub>2</sub>	0.6 eV	0.29 eV	0.2 eV	0.23 eV
E <sub>a</sub>	NO + C <sub>3</sub> H <sub>6</sub> + O <sub>2</sub>	0.53 eV	0.51 eV	0.25 eV	0.3 eV



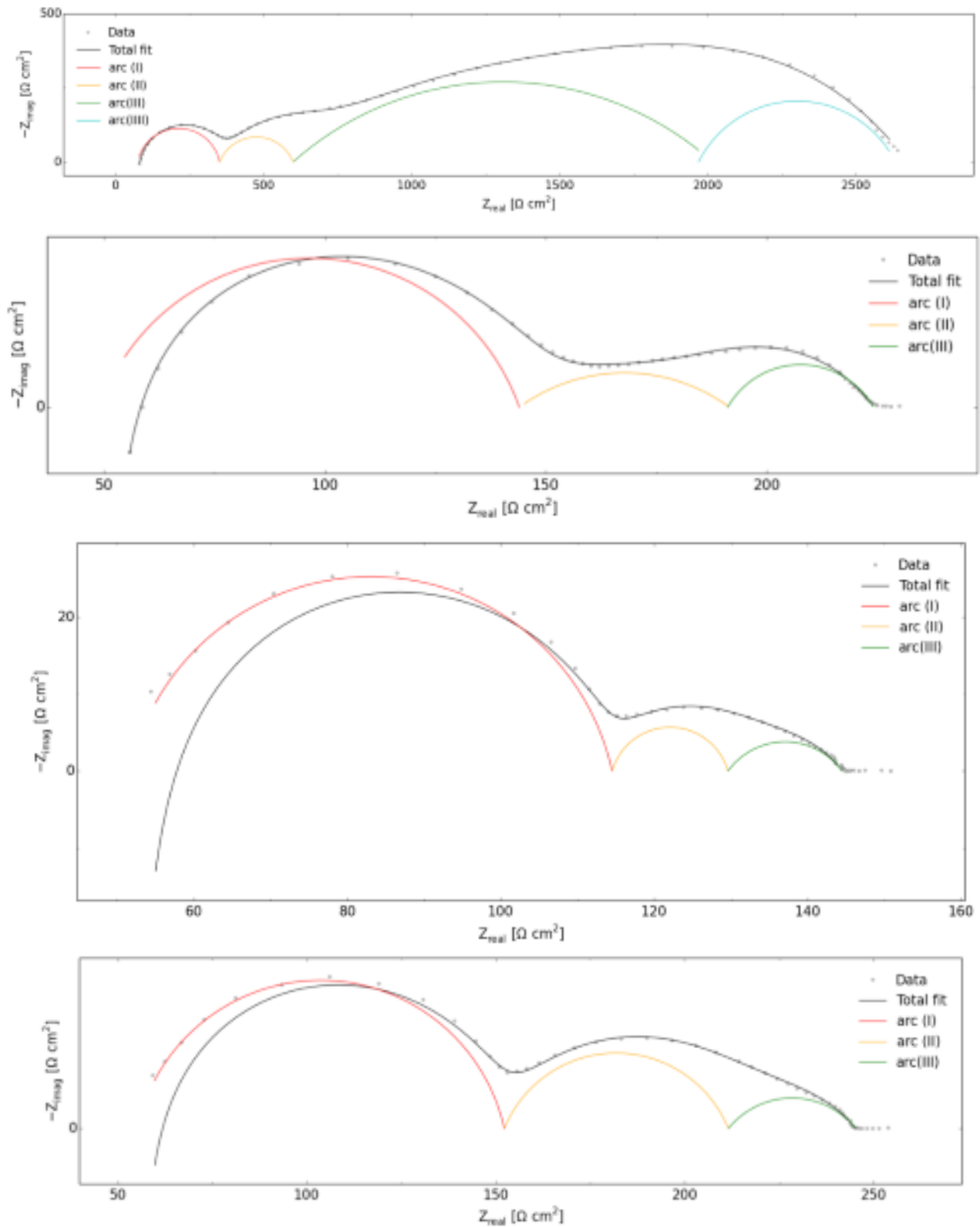


Figure 10. Nyquist plot of impedance spectra obtained on the LSF<sub>15</sub>/CGO<sub>10</sub> porous cell stacks in 1000 ppm NO + 1000 ppm C<sub>3</sub>H<sub>6</sub> + 10% O<sub>2</sub> at 370 °C. Notice the difference in axis. (a) Non impregnated. (b) CPO<sub>20</sub> impregnated. (c) CCO<sub>10</sub> impregnated. (d) Ceria impregnated.

impregnated with CGO<sub>10</sub> showed the lowest polarization resistance, and the non-impregnation cell stack showed the highest at all times. The activation energy for the cells are stated in table 2. The CPO<sub>20</sub> impregnated cell stack was more sensitive to temperature change than the other cells in both atmospheres. The non-impregnated cell showed a big change in E<sub>a</sub> when propene was added and the cell became more sensitive to temperature change. None of the cells showed any signs of degradation during the polarisation as the impedance before and after the test were almost the same.

### 3.3.1. Non impregnated

In figure 10(a) a representative impedance spectrum obtained on the non-impregnated cell stack is shown. The process located at the highest frequency had a high n value and it was well separated from the rest of the spectrum. The activation energy for this arc increased a bit when propene was introduced to the atmosphere (see table 3). The near equivalent capacitance was independent on temperature and atmosphere and had a value of  $1.5 \times 10^{-8}$  F/cm<sup>2</sup>. At 300 °C, in both atmospheres a very small arc could be seen at very high frequency, but it was not possible to fit this arc separately due to overlapping. This caused the C<sub>v</sub> to increase a bit at 300 °C. In the middle frequency region of the spectra a depressed arc (Arc II) with an activation energy of 0.4 eV in 1000 ppm NO + 10% O<sub>2</sub> was found. The near-equivalent capacitance associated with the process decreases with temperature, (see table 4). In 1000 ppm NO + 1000 ppm C<sub>3</sub>H<sub>6</sub> + 10% O<sub>2</sub> the characteristics of the middle frequency arc was similar but with a slightly higher activation energy of 0.5 eV. The third arc (Arc III) obtained on the non-impregnated cell stack in the atmosphere without propene was very difficult to fit because of instability of the system during impedance recording. The size of the arc didn't change that much with temperature but it was not possible to estimate the activation energy of the process. When propene was present, the activation energy of arc III was found to

be 0.46 eV and the near equivalent capacitance decreased very little with temperature and was much higher than the one in the atmosphere without propene (see table 4). A fourth arc was found at high temperature when propene was present in the atmosphere. This low frequency arc had an activation energy of 0.2 eV and the summit frequency and near equivalent capacitance was independent on temperature with values of 0.06 Hz and 0.004 F/cm<sup>2</sup>.

### 3.3.2. CPO<sub>20</sub> impregnation

In figure 10(b) a representative impedance spectrum obtained on the CPO<sub>20</sub> impregnated cell stack is shown. Like in the spectra for the non-impregnated cell stack, a high frequency arc well separated from the rest of the spectrum was found. The activation energy was independent on atmospheres but slightly less than the E<sub>a</sub> obtained on the non-impregnated cell stack. The near equivalent capacitance was affected by a small high frequency arc at 300 °C but otherwise independent of temperature and atmosphere with a value of  $2 \times 10^{-8}$  F/cm<sup>2</sup> (see table 3). The second arc found in the spectra (arc II) had very similar activation energies in the two atmospheres (see table 4) but the C<sub>v</sub> was lower in 1000 ppm NO + 10% O<sub>2</sub> and decreased with temperature. The third arc had the same activation energy in both gasses but C<sub>v</sub> was lower in NO + O<sub>2</sub> and the summit frequency range was larger. The n-value of this arc changed with temperature in the range 0.51-0.6.

### 3.3.3. Ceria and CGO<sub>10</sub> impregnation

The impedance spectra obtained on the ceria and CGO<sub>10</sub> impregnated cell stacks, were very different than the ones from the non-impregnated and the CPO<sub>20</sub> impregnated cells. Figure 10(d) and 1.10(c) shows representative spectra. Even though the polarisation resistance was smaller on the CGO<sub>10</sub> impregnated cell, they looked very much alike. Both of them had a high frequency arc with a low activation energy of 0.27 eV - 0.47 eV (see table 3). The activation

Table 3. Fitting results of the high frequency arc in the impedance spectra in 1000 ppm NO + 10% O<sub>2</sub> and 1000 ppm NO + 1000 ppm C<sub>3</sub>H<sub>6</sub> + 10% O<sub>2</sub>. Capacitances are in [Fcm<sup>-2</sup>], frequency in Hz and activation energy in eV.

		Arc I	
		NO + O <sub>2</sub>	NO + C <sub>3</sub> H <sub>6</sub> + O <sub>2</sub>
Non impregnated	E <sub>a</sub>	0.7	0.8
	C <sub>v</sub>	$1.5 \times 10^{-8}$	$1.5 \times 10^{-8}$
	f <sub>summit</sub>	8155-83241	5253-72381
CPO <sub>20</sub> impregnated	E <sub>a</sub>	0.64	0.63
	C <sub>v</sub>	$3.6 \times 10^{-8} - 2.8 \times 10^{-8}$	$3.3 \times 10^{-8} - 2 \times 10^{-8}$
	f <sub>summit</sub>	14582-135632	11088-117463
CGO <sub>10</sub> impregnated	E <sub>a</sub>	0.27	0.33
	C <sub>v</sub>	$3 \times 10^{-8}$	$2.5 \times 10^{-8}$
	f <sub>summit</sub>	26211-185227	23694-154158
Ceria impregnated	E <sub>a</sub>	0.38	0.47
	C <sub>v</sub>	$2 \times 10^{-8} - 1.7 \times 10^{-8}$	$1.7 \times 10^{-8}$
	f <sub>summit</sub>	24254-167045	18990-145799

Table 4. Fitting results of the two middle frequency arcs in 1000 ppm NO + 10% O<sub>2</sub> and 1000 ppm NO + 1000 ppm C<sub>3</sub>H<sub>6</sub> + 10% O<sub>2</sub>

		Arc II		Arc III	
		NO + O <sub>2</sub>	NO + C <sub>3</sub> H <sub>6</sub> + O <sub>2</sub>	NO + O <sub>2</sub>	NO + C <sub>3</sub> H <sub>6</sub> + O <sub>2</sub>
Non impregnated	E <sub>a</sub>	0.4 eV	0.5 eV	- eV	0.46 eV
	C <sub>v</sub>	$9 \times 10^{-6} - 3 \times 10^{-6}$	$5 \times 10^{-6} - 2 \times 10^{-6}$	$1.5 \times 10^{-4} - 7 \times 10^{-5}$	$2.7 \times 10^{-4} - 1 \times 10^{-4}$
	n	0.74	0.75	0.5	0.47
	f <sub>summit</sub>	24-232	21-421	1.5-2.7	0.1-1.3
CPO <sub>20</sub> impregnated	E <sub>a</sub>	0.42 eV	0.47 eV	0.2 eV	0.2 eV
	C <sub>v</sub>	$1.8 \times 10^{-6} - 3 \times 10^{-7}$	$3.7 \times 10^{-5} - 3.3 \times 10^{-5}$	$0.001 - 3 \times 10^{-4}$	0.007 - 0.002
	n	0.48	0.41	0.51-0.6	0.68
	f <sub>summit</sub>	995-20805	29-133	2.6-17.4	0.43-2.53

energy of this arc increased when propene was added to the atmosphere and it was much lower than the one observed on the non-impregnated and the CPO<sub>20</sub> impregnated cell stacks. The near equivalent capacitances was affected by a small high frequency arc at 300 °C like the other cells, but were otherwise unchanged with temperature. The fitting of the impedance spectra obtained on the ceria and the CGO<sub>10</sub> impregnated cell stacks, could not give a straight line in the Arrhenius plot for Arc II and Arc III. This is due to too much overlapping of the arcs which could not be well separated in the fitting. Therefore the sum of the two arcs has been used to make an Arrhenius plot in figure 10. As can be seen the low frequency part of the spectra is not very sensitive to temperature change, but it had a higher resistance when propene was present in the atmosphere.

## 4. DISCUSSION

### 4.1. NO<sub>x</sub> conversion

Upon polarisation the work function of the electrode is changed. The work function increases when a positive polarisation is applied and the chemisorption of electron donor adsorbate is increased, whereas that of electron acceptors is decreased. Propene is considered an electron donor, and NO and oxygen electron acceptors [25]. The electrode materials, both impregnated and non-impregnated, all act as a catalyst for the NO oxidation into NO<sub>2</sub>. This is seen more on the impregnated cells than on the non-impregnated cell stack. The oxidation into NO<sub>2</sub> is an important step in the NO reduction, since it has been shown to be an intermediate in the reaction according to Werchmeister et al. [19]. When the cells are subjected to positive or negative polarisation, the top electrode is acting as an anode or cathode, respectively. The top electrode is the one exposed to the gas flow and it is assumed that most of the reaction occurs on the top electrode. When the non-impregnated cell stack is subjected to polarisation then the NO oxidation decreases. When the top electrode is a cathode, the oxygen from the gas flow adsorbs on the surface, taking up the catalytic site for NO oxidation. Oxygen is a greater electron acceptor than NO and the chemisorptions is therefore stronger. When the electrode act as an anode, the chemisorption of NO and oxygen is weakened, and the NO is not adsorbed on the surface. When propene is present, the conversion of NO into NO<sub>2</sub> decreases both with anodic and cathodic polarisation. The idea is that the propene should remove the oxygen adsorbed on the surface, to free some active site for the NO molecules. In this work, it seem more like the propene is adsorbing on the surface or the product of propene oxidation (CO) taking up the active sites. No CO was observed in the gas outlet, which points to the former one.

When the CPO<sub>20</sub> and CGO<sub>10</sub> impregnated cells are subjected to polarisation they act differently to the anodic and cathodic polarisation. When the top electrode act as an anode, the behaviour is the same as the non-impregnated cell. When the electrode acts as a cathode, more NO is oxidised, indicating that more NO is adsorbed on the surface. The decrease in the work function increases the chemisorptions of NO and O<sub>2</sub>. The difference from these cells and the one without impregnation is that the O<sub>2</sub> does not take up the active sites for the NO adsorption. This is explained by the increased surface area of ionic conducting material. The absorbed oxygen ions can more quickly be removed from the surface because the three phase boundary is greater. When propene is present

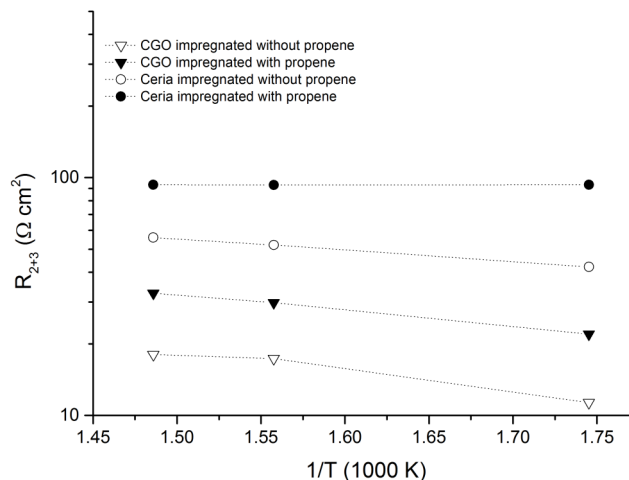


Figure 11. Arrhenius plot of the sum of  $R_2$  and  $R_3$  on the CGO<sub>10</sub> and ceria impregnated cell stacks. Gas feed: 1000 ppm NO + 10% O<sub>2</sub>(open) or 1000 ppm NO + 1000 ppm C<sub>3</sub>H<sub>6</sub> + 10% O<sub>2</sub>(solid)

in the gas flow, NO is still oxidised to NO<sub>2</sub> during cathodic polarisation but in a smaller degree at 300 and 370 °C. At 400 °C the enhancement of the oxidation reaction is higher than without propene, which indicates that the propene is promoting the oxidation reaction. At this temperature the propene might react as expected removing some of the oxygen adsorbed on the surface.

The ceria impregnation does not seem to change anything compared to the non-impregnated cell in the NO + O<sub>2</sub> atmosphere. During cathodic polarisation the O<sub>2</sub> adsorbs stronger than NO taking up active site for NO oxidation, and during anodic polarisation the chemisorption of NO is too weak so less NO<sub>2</sub> is formed compared to the OCV level. When propene is present in the gas stream, the behaviour becomes more like the one for CGO<sub>10</sub> and CPO<sub>20</sub>. The higher surface area seems to increase the propene adsorption. During the cathodic polarisation, the propene might adsorb on the surface and remove some of the many oxygen molecules that has adsorbed, which will increase NO adsorption and hereby the NO oxidation to NO<sub>2</sub>.

### 4.2. Impedance analysis

#### 4.2.1. Effect of impregnation on the cell stacks

The polarisation resistance at OCV for CPO<sub>20</sub> and ceria showed to be very close. Impregnation of LSM<sub>15</sub> electrodes in similar reactors were performed by Ippolito and Hansen [22] and they reported much higher values of  $R_p$  than what was observed in this work. This indicates that the impregnation done in this work was much more efficient. A high frequency arc was recognized in all spectra recorded in both atmospheres on all four cell stacks. For the non-impregnated cell stack and the CPO<sub>20</sub> impregnated cell stack, the size of the activation energy together with the independence of atmosphere suggest that the arc is related to exchange of oxide ions at the interface between electrode and electrolyte [28].

The high frequency arc was different on the CGO<sub>10</sub> and the Ceria impregnated cell stacks even though the near equivalent capacitances were similar. The activation energy was much lower and it was sensitive to propene in the atmosphere. This suggests that the



arc is not only related to the transfer of oxygen ions at the interface between the electrode and the electrolyte. The fact that no adsorption related arc was found in the spectra indicates that the impregnation material decreased the resistance of this process and it became too small to observe in the spectra due to overlapping with other processes. The impedance response of a process that is related to adsorption and dissociation of oxygen will be dependent on atmosphere. Therefore the high frequency response on the CGO<sub>10</sub> and ceria impregnated cell stacks, could be a mixture of these two processes. The low frequency response on the non-impregnated cell stack was very sensitive to propene being present in the atmosphere. The magnitude and summit frequency in NO + O<sub>2</sub> showed no dependency of measurement temperature. These observations suggest that the origin of this arc is gas diffusion [28]. In the work of Ippolito and Hansen [29] a large change in the impedance response was seen on a LSF<sub>15</sub>/CGO<sub>10</sub> cell stack, when it was exposed to 10% O<sub>2</sub> versus 1000 ppm C<sub>3</sub>H<sub>6</sub> + 10% O<sub>2</sub>. The effect of propene was seen in the low frequency response of the impedance increasing the R<sub>p</sub> significantly. They explained the low frequency response to be due to strong competition between propene adsorption on the electrode surface with the adsorption and the dissociation of oxygen, and the arc was ascribed to dissociation and surface diffusion of oxygen species on the electrode.

On the ceria and CGO<sub>10</sub> impregnated cell stacks, the middle frequency and the low frequency arcs did not show any temperature dependence and the resistance of the processes were higher when propene was present. The lack of temperature dependence could suggest either gas diffusion impedance or gas conversion impedance [30],[31]. The dependence on propene being present in the gas, could suggest a kind of conversion that propene inhibits. In the work of Werchmeister et al. [18], the arc observed at low frequency was ascribed to conversion of intermediately formed NO<sub>2</sub>. When propene was present in the atmosphere less NO was oxidised to NO<sub>2</sub> at OCV and the level of NO was at all temperatures higher than the level of NO<sub>2</sub>. This can explain the increase in resistance of a process at low frequency that involves the NO<sub>2</sub> when propene is present.

The CPO<sub>20</sub> impregnated cell stack behaved much differently than the others. The middle frequency arcs found in the spectra both with and without propene were similar in activation energy but the C<sub>v</sub> and summit frequency differed. These suggest that the arcs represent two different processes. In NO + O<sub>2</sub> the near equivalent capacitance decreased with temperature but when propene is present it is independent of temperature.

## 5. CONCLUSION

In the present work, the effect of Ceria, CGO<sub>10</sub> and CPO<sub>20</sub> impregnation on the NO reduction by propene on LSF<sub>15</sub>/CGO<sub>10</sub> electrodes was investigated. For this an electrochemical cell stack consisting of 11 alternating layers of electrolyte and electrode was used. It was clear that the impregnation of nanoparticles enhanced the catalytic activity of both propene oxidation and NO reduction into nitrogen with propene as the reducing agent. Also the oxidation on NO into NO<sub>2</sub> was increased. The application of a potential to the cell stacks, did not show any enhancement of the reduction of NO into nitrogen with or without the presence of propene. The electrochemical enhancement of propene oxidation was quite low, and the conversion increased from 75% to 77% at 400 °C on a ceria

impregnated cell. The CGO<sub>10</sub> and CPO<sub>20</sub> had similar conversions. The non impregnated cell only converted 7% of the propene at the same temperature without any electrochemical enhancement.

However the NO oxidation to NO<sub>2</sub> was greatly affected by the application of a potential. The conducting properties of the impregnation material, showed to be important for this reaction. A high ionic conductivity seems to promote NO adsorption because the adsorbed oxide ions are removed faster from the surface via the increased three phase boundary. These properties do not seem to be important to the adsorption of propene which increases when the surface area of the electrode is increased.

Impedance investigation of the cells revealed a lower polarisation resistance of the impregnated cells compared to a cell without impregnation. The introduction of propene into the atmosphere increased the polarisation resistance of all the cells. However, only processes related to adsorption were affected by the presence of propene. The impedance response of the cells impregnated with Ceria and CGO<sub>10</sub> showed a great reduction of the resistance of an adsorption process participating in the charge transfer reaction. However, the adsorption species is not identified and could be NO as well as oxygen and propene. A gas conversion process involving NO<sub>2</sub> showed to be inhibited by propene which led to a higher resistance of the process.

The CPO<sub>20</sub> impregnated cell showed a different impedance response, suggesting that different processes are occurring on the material but in this work the processes were overlapping too much for identification to be possible.

## REFERENCES

- [1] N. Imanaka and T. Masui, Appl. Catal. A-Gen., 431, 1 (2012).
- [2] T. Huang, CY. Wu, S. Hsu and C. Wu, Appl. Catal. B-Environ., 110, 164 (2011).
- [3] M. Iwamoto and H. Hamada, Catal. Today, 10, 57 (1991).
- [4] T. Harada, S. Kagawa and Y. Teraoka, Appl. Surf. Sci., 121-122, 505 (1997).
- [5] R. Zhang, A. Villanueva, H. Alamdari and S. Kaliaguine, Appl. Catal. A-Gen., 307(1), 85 (2006).
- [6] K.K. Hansen, E.M. Skou, H. Christensen and T. Turek, J. Catal., 199(1), 132 (2001).
- [7] S. Pancharatnam, R.A. Huggins and D.M. Mason, J. Electrochem. Soc., 122(7), 869 (1975).
- [8] X. Tang, X. Xu, H. Yi, C. Chen and C. Wang, Sci. World J., 2013 (2013).
- [9] S. Bredikhin, K. Hamamoto, Y. Fujishiro and M. Awano, Ionics, 15 (3), 285 (2009).
- [10] K.K. Hansen, Appl. Catal. B, 58(1-2), 33 (2005).
- [11] K.K. Hansen, Appl. Catal. B Environ., 100(3-4), 427 (2010).
- [12] R.M.L. Werchmeister, K.K. Hansen and M. Mogensen, J. Solid State Electrochem., 16(2), 703 (2012).
- [13] K.K. Hansen, E.M. Skou and H. Christensen, J. Electrochem. Soc., 147(5), 2007 (2000).
- [14] K.K. Hansen, Electrochem. Comm., 9(11), 2721 (2007).
- [15] K.K. Hansen, Electrocatal., 5(3), 256 (2014).
- [16] K.K. Hansen and E.M. Skou, Solid State Ionics, 176(9-10), 915 (2005).

- [17]R.M.L. Werchmeister, K.K. Hansen and M. Mogensen, *Maters. Res. Bull.*, 45(11), 1554 (2010).
- [18]R.M.L. Werchmeister, K.K. Hansen and M. Mogensen, *J. Electrochem. Soc.*, 157(12), 107 (2010).
- [19]R.M.L. Werchmeister, K.K. Hansen and M. Mogensen, *J. Electrochem. Soc.*, 157(5), 35 (2010).
- [20]K.K. Hansen and M. Mogensen, *ECS Trans.*, 13(26), 153 (2008).
- [21]D. Ippolito, K.B. Andersen and K. Hansen, *J. Electrochem. Soc.*, 159(6), 57 (2012).
- [22]D. Ippolito and K.K. Hansen, *J. Solid State Electr.*, 17(3), 895 (2013).
- [23]K.B. Andersen, F.B. Nygaard, Z. He, M. Menon and K.K. Hansen, *Ceram. Int.*, 37(3), 903 (2011).
- [24]Elechemea analytical. <http://www.elchemea.com>, 2012. Accessed : 2014-07-08.
- [25]C.G. Vayenas, S. Brosda and C. Pliangos, *J. Catal.*, 203(2), 329 (2001).
- [26]B. Beguin, F. Gaillard, M. Primet, P. Vernoux, L. Bultel, M. Henault, C. Roux and E. Siebert, *Ionics*, 8(1-2), 128 (2002).
- [27]F.C. Buciuman, E. Joubert, J. Barbier and J.C. Menezes, *Appl. Catal. B-Environ.*, 35(2), 149 (2001).
- [28]M.J. Jorgensen and M. Mogensen, *J. Electrochem. Soc.*, 148(5), A433 (2001).
- [29]D. Ippolito and K.K. Hansen, *J. Electrochem. Soc.*, 161(3), F323 (2014).
- [30]S. Primdahl and M. Mogensen, *J. Electrochem. Soc.*, 145(7), 2431 (1998).
- [31]M.B. Mogensen, *J. Electrochem. Soc.*, 146(8), 2827 (1999).